Chapter 5

Multifunctional Graphene Oxide Implanted Polyurethane Ionomer Gel Electrolyte for Quantum Dots Sensitized Solar Cell

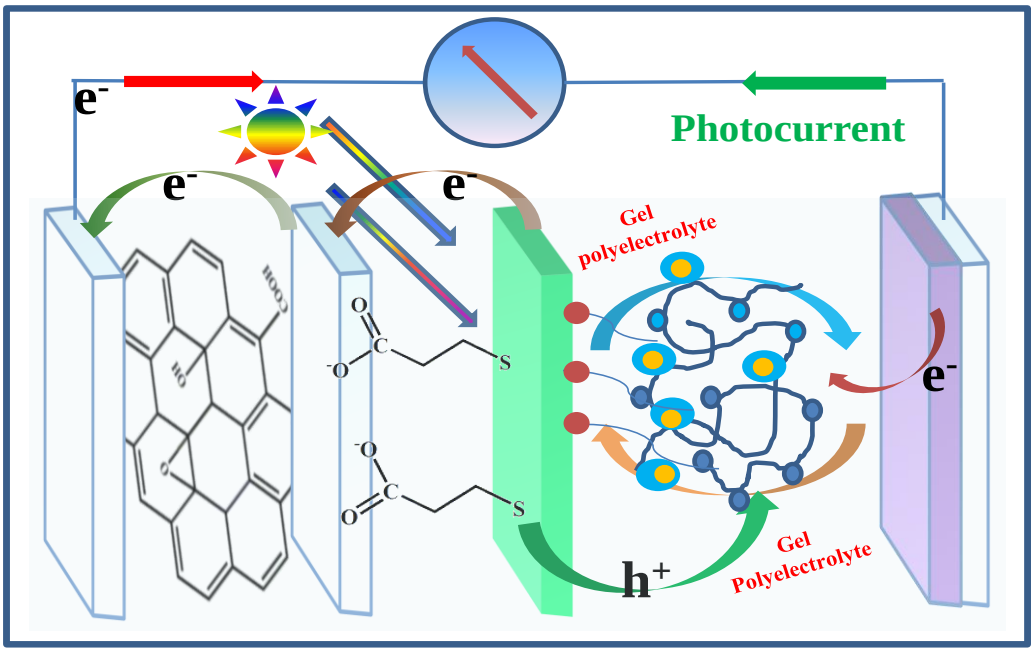

5.1. Introduction

Renewable energy from cheaper green sources is a reasonable solution for the global energy crisis [176]. Quantum dot sensitized solar cells are emerging technology for the absorption and conversion of solar energy into electrical energy based on photo electrochemical reaction of redox electrolyte [177,178]. Electrolyte acts as bridge which offers faster charge conversion and transmission between photoanode and photocathode. A well active electrolyte possesses high intrinsic conductivity to facilitate better photo conversion phenomenon in solar device. Photovoltaic devices that utilize a liquid electrolyte have the potential for other problems, including leakage, volatility, flammability, and quantum dot corrosion [90]. The use of quasi-solid-state gel electrolytes creates critical issues: reduced charge-transfer rate and sluggish electrocatalytic behaviors at counter electrode/gel electrolyte interfaces. However, interconnected conducting channel offers short charge transfer length and expanded electrocatalytic area for electrolyte active species. Duan et al. developed graphene implanted polyacrylamide (PAAm-G) conducting polymer gel electrolytes for QDSSCs with a power conversion efficiency of 2.34% [67]. Jin et al. developed PAAm/GO gel electrolyte for QDSS cell with energy conversion efficiency of 4.10% in comparison with 1.78% without incorporating GO [66]. Suggesting that GO tailored conducting gel electrolyte facilitates conversion of S_n^{2-} to S^{2-} which in turn leads to enhancement of photoexcited electron density at photoanode. Sodium polyacrylate (PAAS) or sodium carboxymethylcellulose (CMC-Na) was employed into polysulfide electrolyte [78,89]. Highly efficient and stable quasi-solid-state quantum dot-sensitized solar cells based on a superabsorbent polyelectrolyte Sun et al. utilized functional PEG additive for polysulfide electrolyte to improve photovoltaic performance in QDSS cell [179]. This leads to improvement of absorption and retention of liquid electrolyte through porous network. The SiO_2 and tetraethylorthosilicate (TEOS) additives have been used

in polysulfide electrolytes to create an energy barrier that efficiently restrains photo-generated electron recombination between the photoanode and electrolyte [84,180]. Moreover, the defects or oxygen-containing groups located at the edge site can act as active sites for electrocatalytic reaction in electrolyte [181,182]. The application of superabsorbent polyelectrolyte as gel electrolyte provides a new approach for construction of quasi-solid-state QDSCs. Polyelectrolytes bearing electrolyte groups are charged polymer having own hydrophilic groups and 3D framework. The structural integrity offers superabsorbent, wettability and excellent electrical conductivity [183]. In other words, Polyelectrolyte contains charged chemical moieties which itself functions as oxidizing as well as reducing component. Polyurethanes are composed of hard segment and soft segment in a block copolymer fashion**.** Sulfonation improves electrical properties of graphene oxide implanted polyurethane chain because of insertion of hydrophilic group (pendant anion) as well as presence of deprotonated carboxylate group [175]. Electrolyte functional group controls the charge recombination phenomenon [184]. Gel polyelectrolyte activity is due to presence of electrochemical active polar group such carboxylate or sulfonate moieties in their host structure [185]. Different additives containing functional end-groups can be used to chemically modify the electrolyte and its interface with the photoanode and counter electrode.

In this work, multifunctional graphene oxide implanted polyurethane ionomers have been developed as solvent swollen gel polyelectrolytes for Quantum dot sensitized solar cell. Electrolyte active group ($-CH_2-CH_2-CH_2-SO_3^- Na^+$) has been embedded in the hard segments of the polyurethane backbone. In practice, the counterion (Na^+) resides on polar functionalities which support electrical conducting behaviour. Here, gel polyelectrolyte has been realized without incorporation of additive or liquid polysulfide electrolyte. Multifunctional activity can be

created in electrolyte structure via reaction or insertion of specific functional group and via conversion of some integral functionality. Polyelectrolyte activity is due to presence of chemically different redox active phase as integral part of the electrolyte. The hard segment functionalized polyurethane ionomers are expected to functions as redox responsive components as well as passivation layer for efficient photovoltaic reaction. Pendant anion (propane sulfonate) not only resides on polyurethane chain but also react with active functional components of graphene oxide. The optimum GO content facilitates the electrolyte activity of polyurethane ionomer. The presence of oxygenic functionalities causing enhanced surface activity with photoanode and counter electrode. However, high content of GO screens the redox activity of electrolyte active pendant anion. Moreover, electrolyte active rich charged polymers will definitely boost the photovoltaic performance of QDSSCs. It should be explored that the present idea provides a new innovation for boosting PCE of QDSSCs.

5.2. Results and discussion

5.2.1. Structural and functional impact of pendant anion on GO functionalized polyurethane chain

Functionalization scheme of poly (urethane-urea) (PU) has been shown in **(Scheme 5.1)**. Polyurethane ionomer (PUI) consists of multiple oxygenic functionalities and electrolyte active group at different chemical (urethane and urea linkages) environment. Pendant anion bearing redox active hard segments works as electrolyte active components while electron rich oxygenic functionalities works as surface passivation group. Pendant anion lowers the activation and surface energy of polyurethane chain. Actice $-SO_3^-$ are responsible for redox activity and reversible change. Thus, polyurethane ionomer contains functionalized hard segments and oxygenic soft segment with their different activity in same extended platform (chain).

Synthesis of multifunctional graphene oxide implanted polyurethane chain with content of 0.5% GO result in considerable variation of chemical structure. Two chemically different urethane linkages (first, due to reaction of PTMG with HMDI) and second one, correspond to reaction of NCO – terminated prepolyurethane with active hydroxyl component of graphene oxide. In consequence, ionomer phase has been produced by chemical incorporation of ϒ – propane sultone in the presence of sodium hydride into resultant polyurethane chain **(Scheme 5.2).** Sodium cation not only works as counter ion on electrolyte active group but also adsorbed on polar functionalities of the polyurethane chain. The resultant Functionalized polyurethane composite ionomer possess two different electron en-rich pendant groups as integral components on different chemical environment.

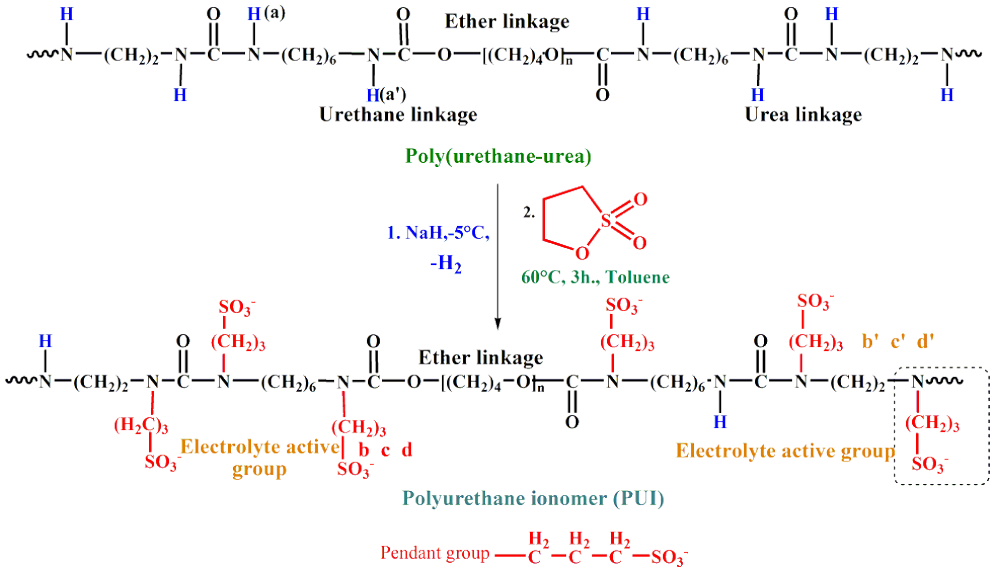

Scheme 5.1. Schematic presentation of Polyurethane ionomer (PUI) bearing electrolyte active groups

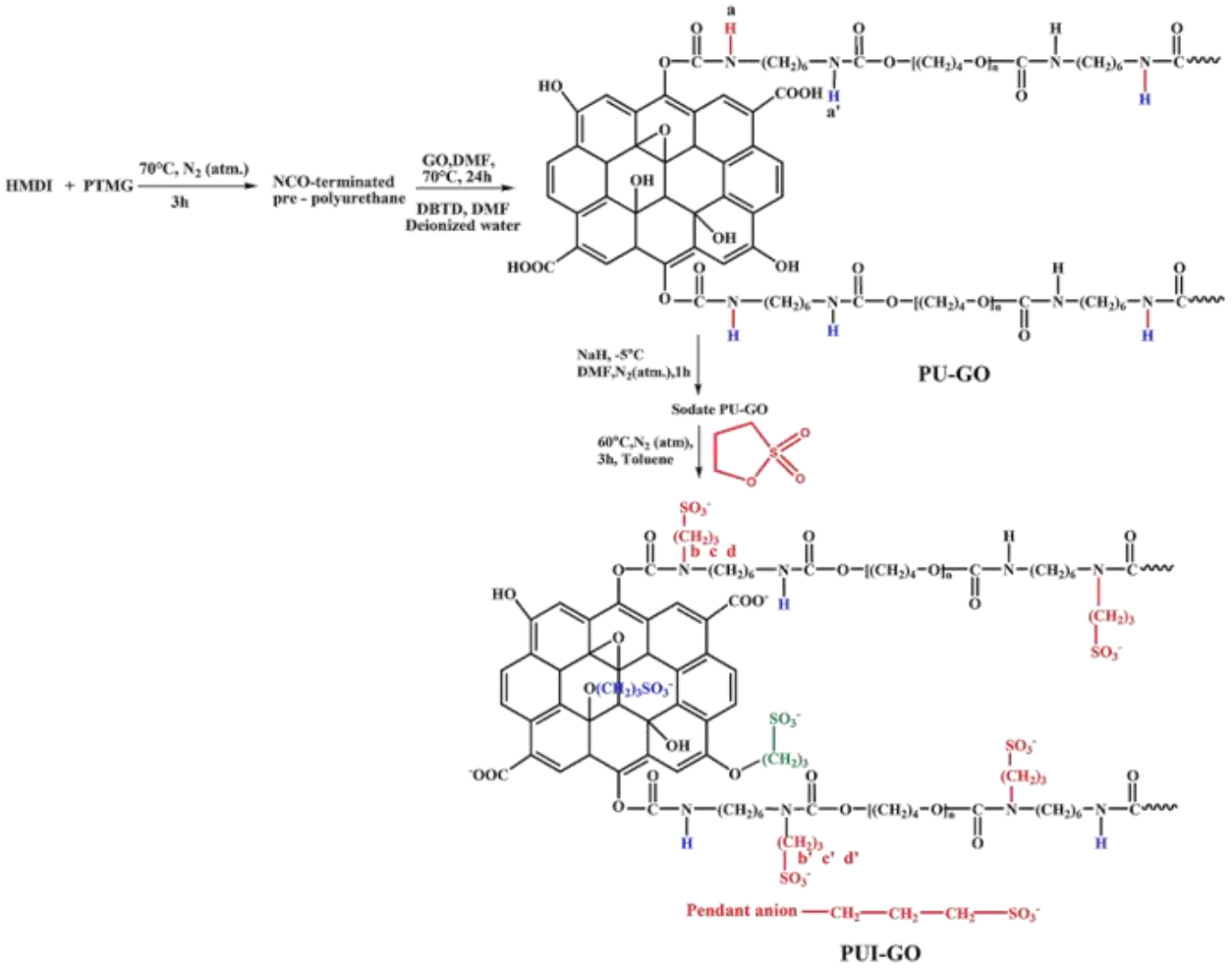

Scheme 5.2. Schematic reaction pathway for synthesis of multifunctional Graphene oxide implanted Polyurethane ionomer.

Pristine poly (urethane –urea) showed two peaks at 8.20 ppm (more hydrogen bonded urea-NH leveled as a) and 7.04ppm (urethane-NH leveled as a'). The peak due to urethane proton was found to be absent in PUI. But a peak at 8.32 ppm confirms the chemical atmosphere of pendant anion in urea linkage of PU chain.

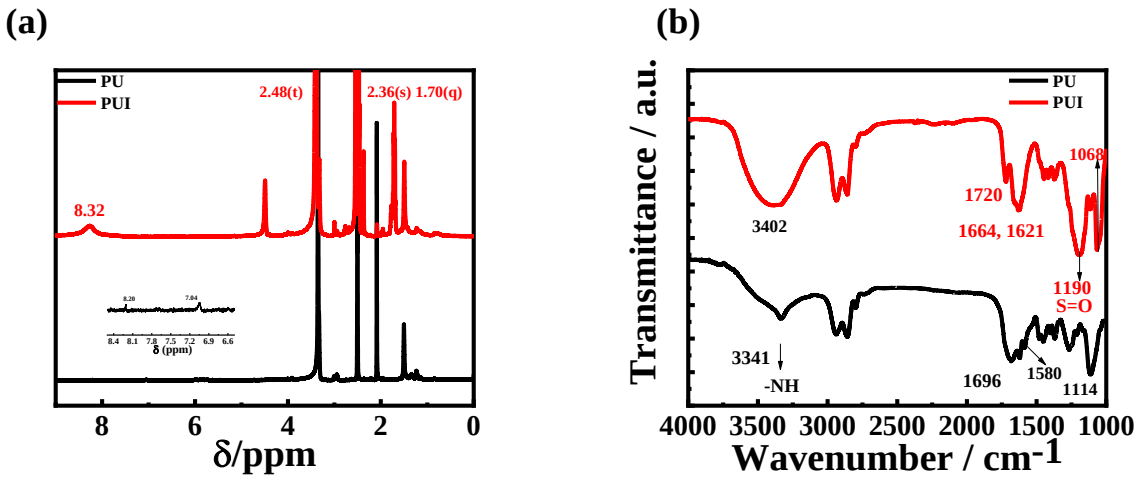

Figure 5.1 (a) ^{1}H NMR spectra of pristine poly (urethane-urea) and polyurethane ionomer (PUI). (b) FTIR spectra of poly (urethane-urea0 and its ionomer.

The formation of chemically implanted graphene oxide nanohybrid (PU-GO) has been confirmed from NMR spectroscopy arising from the new peak at δ = 7.95 ppm at lower field due to >N−H proton (leveled a) adjacent to the linked bulky GO sheet. However, ^{1}H signal for regular >N−H (leveled a') groups present in urethane linkages appears at δ = 7.03 ppm for GO linked PU chain. One peak at 7.85 ppm attributed to aromatic ring proton of GO linked polyurethane. The resonance effect (structure) shields the NH proton in urethane linkage result in lower chemical shift than the urea-NH. GO reduces the electron density around urethane group causing de-shielding than the pristine urethane. However, regular urethane-NH proton peak disappeared in PUI-GO but a shifted peak at 7.81 ppm confirms the presence of propane sulfonate group in urethane linkage adjacent to GO sheet. Pristine urethane- CH_2 (3.44 ppm) shifted towards higher value (3.71 ppm) confirming the presence of pendant anion. Thus, pendant anion incorporated urethane linkage reduces the extent of intermolecular H-bond. In addition, three distinct CH_2 (b c d and b' c'd') protons showed different value of chemical shift in PUI-GO confirming the attachment of propane sulfonate in hard segments (pristine urethane

linkage and urethane linkage due to linked GO sheet) of PU-GO chain. Thus, GO intensifies the extent of pendant anion on urethane linkages.

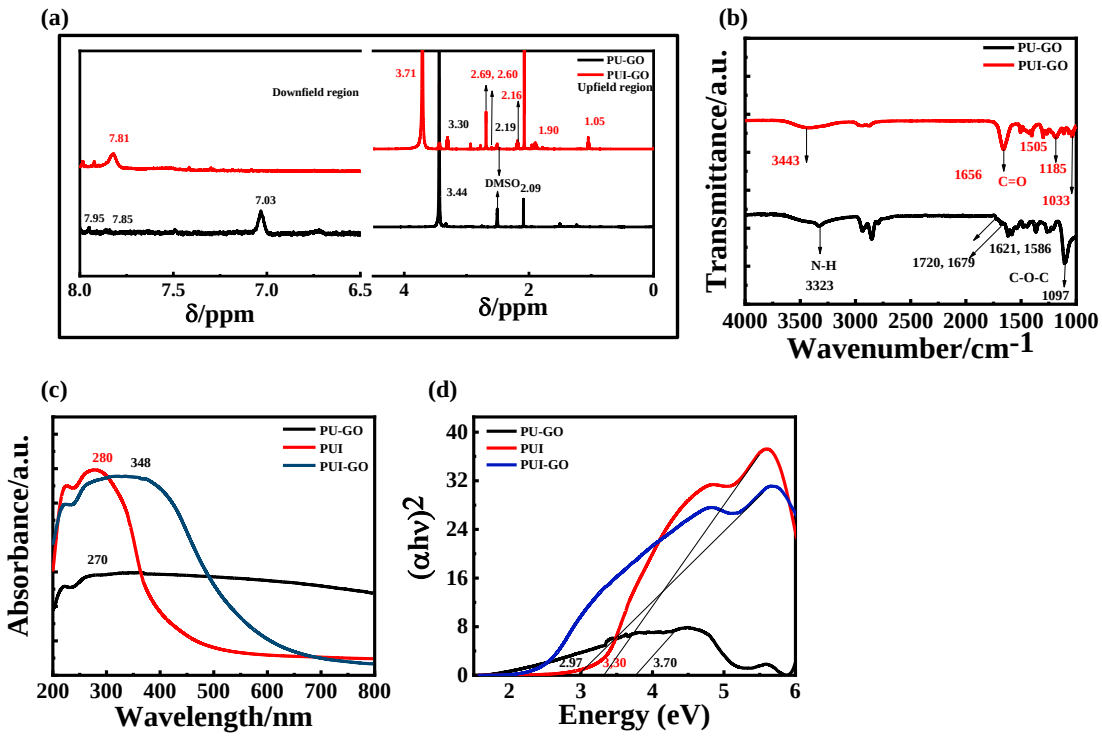

Figure 5.2: (a) Solution state 1H NMR spectra of PU-GO and PUI-GO showing spectral peaks in downfield and upfield regions. (b) Solid state FTI spectra of PU-GO and PUI-GO showing specific and characteristic peaks. (c) Solid state UV-visible absorption spectra of PU-GO, PUI and PUI-GO showing shifted red shifted absorption band. (d) Tauc's plot for investigation of energy gap and structural confinement effect.

In FTIR spectra, PU and PUI-GO showed characteristic peaks at 3341 and 3323 cm^{-1} confirming the presence of -NH group in hard segments [186]. PU are capable of forming several kinds of hydrogen bonds due to the presence of a donor N-H group and a C=O acceptor group in the urethane linkage [187]. However, PUI and PUI-GO showed shifted absorption peaks at 3402 and 3443 cm^{-1} for NH group. The data indicates that GO reduces the extent of Hydrogen bonding between interchains of polyurethanes. PU showed merged absorption peak at 1696 cm^{-1}

(C=O) while PU-GO exhibited characteristic peaks at 1720, 1679 confirming the presence of CO group due to carboxylic group tagged in GO and urethane linkages in hard segments. The CO absorption peaks spilitted into two closely spaced peaks (1720, 1664 cm^{-1}) with shoulder in PUI and one unique peak (1656 cm^{-1}) in PUI-GO. GO improves the interaction of propane sulfonate (pendant anion) into urethane linkages. The lower value of CO frequency demonstrates enhanced adsorption of Na^{+} over CO group and carboxylate group. PUI and PUI-GO exhibited characteristic unique peaks at 1190 and 1185 cm^{-1} indicating the presence of S=O group functionalized hard segments. The intensity of S=O band (peak) increases with an increase in the content of pendant anion from ϒ – propane sultone group. The absorption peaks at 1068 and 1033 cm^{-1} confirms the presence of C-O-C group in PUI- and PUI-GO, respectively. The lower C-O-C frequency indicates that GO enhanced the interaction of pendant anion and hence counter ion (Na^{+}) on polar oxygenic groups. Thus, GO enriches the pendant anion into polyurethane chain because of its electron withdrawing nature adjacent to urethane linkage.. The increased repulsive interaction resulting from carboxylate anion or sulfonate anion makes the ionomer more expanded structure [188].

In UV-visible absorption spectra, polyurethane ionomer showed enhanced absorption because of presence of electrolyte active chromophore. Pristine polyurethane ionomer (PUI) showed a absorption band (224 nm, π-π* transition) and broad band (280 nm, n-π* transition). PU-GO showed absorption band at 217 nm and 270 nm due to structural confinement and electronic redistribution. In other hand, absorption band 221 nm and expanded absorption band at 348 nm have been developed in PUI-GO. The broad n-π* transition is due to enhanced absorption which is primarily due to increased reactivity of urethane linkages towards propane sultone. Thus, GO improves the transition and absorption capacity into resulting polyurethane

ionomer. The band gaps are obtained as 3.70, 3.30 and 2.97 nm for PU-GO, PUI and PUI-GO due to absorption edge transition.

5.2.2. Thermal and structural stabilization characteristics

The initial weight loss was accelerated in TGA curve of GO (0.5%) implanted polyurethane due to the pyrolysis of the labile oxygen-containing functional groups. However, PUI and PUI-GO showed little lower thermal stability due to moisture absorbing nature. The degradation temperature 217°C, 240° and 281°C were assessed at 5% weight loss for PUI-GO, PUI and PU-GO. PUI showed little higher thermal degradation because of two different hard segment content (urethane and urea linkages). First stage degradation seems faster due to enhanced hydrophilic content and urethane linkages in PUI-GO. Polar oxygenic entities are more susceptible towards heat absorption. Second stage degradation remains almost constant for wide range of temperature confirming thermos-oxidative stability (barrier effect of GO) as compared to pristine polyurethane ionomer (PUI). Polyurethane ionomer showed faster degradation. Moreover, GO prevents weight loss in complex structure of polyurethane ionomer. Maximum decomposition temperature increased little bit in PUI-GO. Thus, synergistic interaction of GO, polar pendant anion, PU hard segments contributed to the heat resistance performance. The complexation and interaction inside the polyurethane chain leads to decreases the crystallinity and softened the backbone of polymeric content[189].

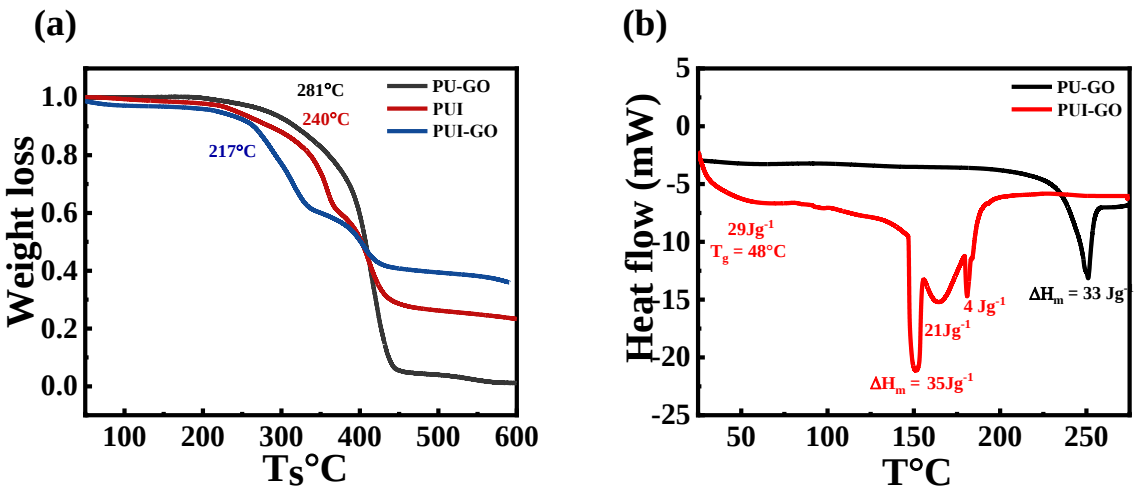

Figure 5.3: (a) TGA curves of PU-GO (0.5%), PUI and PUI-GO (0.5%). (b) DSC thermogram of PU-GO (0.5%) and its ionomer (PUI-GO)

PU-GO showed sharp melting (melting endotherm) at 251°C with melting enthalpy of 33Jg^{-1} in onset temperature range (243°C-254°C) in DSC curve. However, PUI-GO showed glass transition temperature 48°C due to thermal transition indicating the presence of segmental mobility. The structure contains amorphous phase. In practice, PUI-GO showed triple bottom thermal transition (endotherms) with melting temperature at 150°C (35 Jg^{-1}), 164°C and 181°C. The complete triple bottomed thermal transition showed thermal enthalpy of 212 Jg^{-1} in the onset temperature range of (147-155°C). The triple bottomed thermal transition is attributed to different chemical atmosphere and synergistic interactions in the presence of pendant anion.

5.2.3. Morphological and structure-function characteristics

TEM micrograph demonstrates that the small electrolyte active guest is not likely to reside in the internal core since it is charged, and instead it may prefer the periphery of the core-shell structure. Chemically tagged GO encapsulated through polyurethane hydrophobic chain and resembles dispersed in the matrix. GO remain stacked and uniformaly distributed throughout the polyurethane ionomer chain[190]. Electrolyte active embedded structure contains lowest energy almost spherical size (35 nm). AFM micrograph clearly depicts the root mean square roughness

of the surface structure. PU-GO showed a roughness value of 10 nm in contrast to roughness value of 6 nm in case of PUI-GO. The roughness value decreases once the electrolyte active pendant anion is embedded into the polyurethane chain. It resembles that PUI-GO best suited to chemical wettability

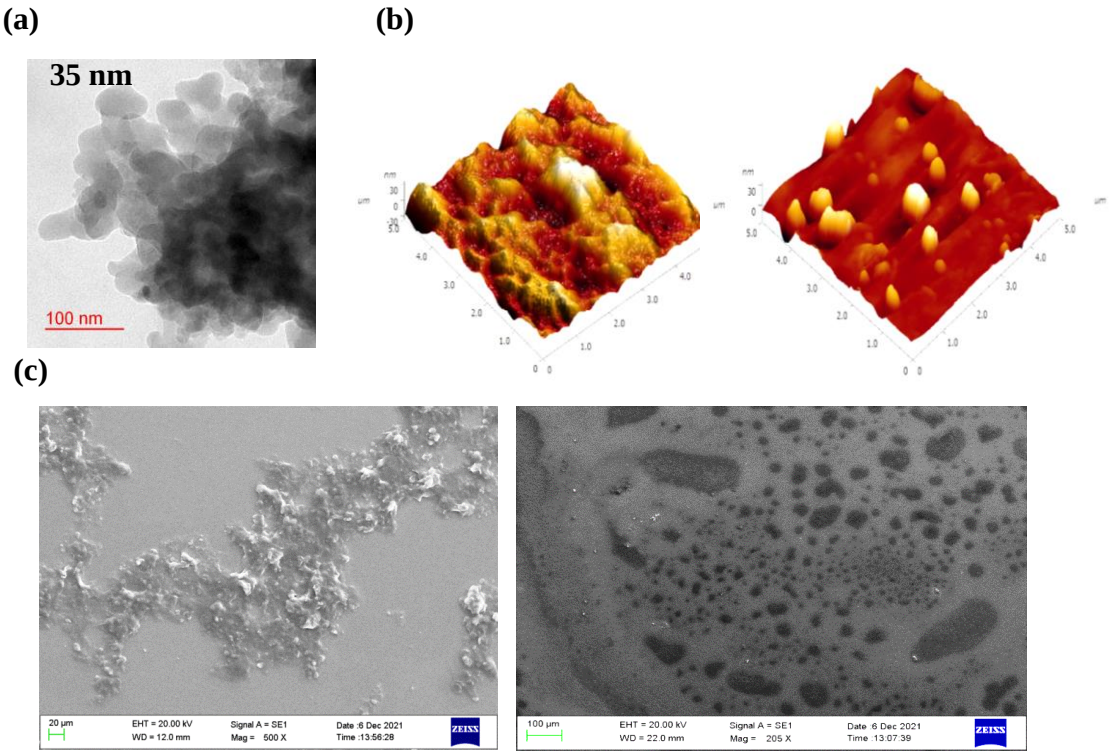

Figure 5.4: (a) TEM image of PUI-GO (0.5%). (b) AFM image of PU-GO (0.5%) and PUI-GO (ionomer) film spin coated on silcon wafer. (c) SEM image of PU-GO (0.5%) and PUI-GO

5.2.4. Electrochemical and structure-function characteristics

Figure 5.5a reports electrochemical cyclic voltammetry measurements. PU-GO showed onset oxidation potential at 0.381V while onset reduction potential was observed - 0.058V. However, it may be noted that we observed no voltammetry intense signal for pure polyurethane solution as they are electrochemically inactive in scanned electrochemical window. PUI-GO exhibited onset oxidation at 0.600V and onset reduction at -0.621V. In contrast, pristine polyurethane

ionomer (PUI) showed onset oxidation potential at 0.73V. Moreover, functionalized polyurethane ionomer show good redox behaviour because of presence of pendant anions on hard segment content as well as graphanic plane of implanted graphene oxide. Thus, polyurethane ionomer consisted of electrolyte active hydrophilic group which provides reversible electrochemical activity. 0.2% GO implanted polyurethane ionomer showed onset oxidation at 0.70V while 1% GO implanted polyurethane ionomer showed onset oxidation at 0.76V. High content of GO further stabilize the oxidation level in composite ionomer. The oxidation potential variation can be attributed to the changes in the polyurethane framework of the π-bridge (condensed ring) moiety.

Figure 5.5b displays EIS measurements for PU-GO, PUI, and PUI-GO (0.5%). The solutions were scanned in the range of 0.1Hz. to 1MHz at amplitude of 0.01Vrms operated at room temperature. EIS measurement showed that PU-GO shows large semicircle with ionic conductivity of 18×10^{-5} S/cm. However, polyurethane ionomer showed spike with ionic conductivity value of 1×10^{-3} S/cm. Similarly, PUI-GO (0.5%) showed spike with enhanced ionic conductivity of 4.48×10^{-3} S/cm. Ionic conductivity was intensified due to combined effect of electrolyte active group in different chemical environment. This is probably due to imbibition of electrolyte active pendant anion in conducting channel of polyurethane PU-GO.

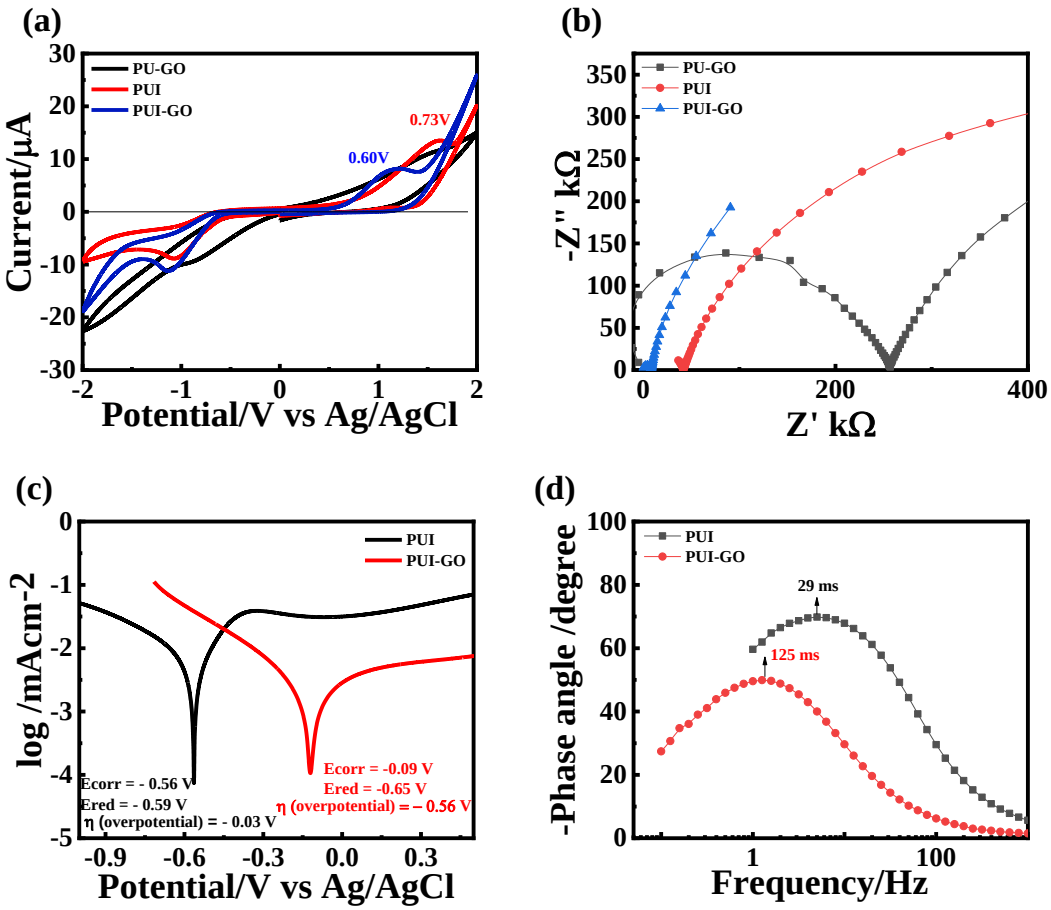

Figure 5.5: (a) Solution phase cyclic voltammetry of PU-GO (0.5%), Pristine PUI and PUI-GO recorded at room temperature with scan rate of 20 mV/s. (b) Electrochemical impedance spectroscopy (EIS) of PU-GO (0.5%), PUI and PUI-GO (0.5%). (c) Tafel plot for the investigation of electrocatalytic activity and corrosion inhibition. (d) Bode plots for the investigation of lifetime of free electron on the surface of electrolyte active group) in PUI and PUI-GO (0.5%).

Polyelectrolyte	E_{red}(V)	E_{ox}(V)	ΔE_p(V)	E_{HOMO} (eV)	E_{LUMO} (eV)
PUI	-0.59	0.73	1.32	-5.13	-1.85
PUI-GO (0.2%)	-0.67	0.70	1.37	-5.10	-1.83
PUI-GO (0.5%)	-0.65	0.60	1.25	-5.00	-2.09
PUI-GO (1.0%)	-0.58	0.76	1.34	-5.16	-1.65

Table 5.1 Estimation of electrochemical parameters and characteristic values from cyclic voltammetry for polyelectrolyte solutions

Figure 5.5c shows tafel plots for PUI and PUI-GO (0.5%). Tafel plots were recorded for investigation of E_{corr} and electrocatalytic activity due to interfacial contact of Pt counter electrode. The solution phase electrochemical characteristic values and onset peak to peak separation potentials (ΔE_p) have been shown in **Table 1**. The lower value of ΔE_p (1.25V) accelerates the electrocatalytic reaction. The E_{corr} were estimated as -0.56V and -0.09V for PUI and PUI-GO (0.5%) respectively. The negative E_{corr} value confirming the non corrosive behaviour of polyelectrolyte. The calculated overpotential (η) was observed as -0.03V and -0.56V for PUI and PUI-GO (0.5%). Greater negative overpotential demonstrated faster electrocatalytic activity as compared to lower negative overpotential (PUI). The high electrocatalytic activity is due to presence of more electrocatalytic sites [191] or electrochemical area on the surface of PUI-GO. This is primarily because of low surface energy which ultimately undergoes fast electrocatalysis. The conductive Pt easily dopes the deficient surface.

Figure 5.5d reports Bode plots for the determination of free electron lifetime. The electron lifetimes (τ_n) can be estimated according to the equation $\tau_n = 1/2\pi f_{max}$, where f_{max} is the maximum frequency of the lower-frequency peak in the Bode phase plot. Peak frequency is inversely proportional to the electron lifetime value. Photoexcited electron lifetime can be monitored through engineering of electrolyte structure. The lifetime of electrons involved in oxidized electrolyte active group reduction depends on the structural channel linked on polyelectrolyte. Electrolyte prolong the lifetime of photoexcited electron for efficient conversion. Pristine PUI showed electron lifetime 29 ms while GO implanted PUI exhibited longer lifetime (125 ms). The higher lifetime stabilized the photoexcited surface of QDs. Polyelectrolytes having higher lifetime can reduce the surface charge recombination and extend the lifetime in excited state of QDs. Higher lifetime supported electrolyte structure may increase the open circuit

potential [192]. GO implanted polyelectrolyte supports to improve open circuit potential because of synergistic activity (electrolyte as well as passivation phenomenon).

5.3. MPA functionalized QDs, functional structure and size quantization effect

Figure 5.6a represents the FTIR spectrum of free CdS and 3-MPA capped CdS quantum dots. The band emerged at 634 cm-^{1} corresponding to the stretching vibration of free CdS. As The peaks at 1554 cm^{-1} and 1394 cm^{-1} were assigned to vibrational modes of asymmetric and symmetric stretching vibrations of carboxylate (COO^{-}) group of 3-MPA molecules in caped CdS. 3-MPA molecule is successfully capped with the CdS. The characteristic absorption peak at 1710 cm^{-1} is due to CO group of carboxylate ion on the surface of CdS. The characteristic C–S band of 3-MPA-capped CdS was observed 1442 cm^{-1}. One additional peak at 2969 cm^{-1} was assigned for stretching vibration of $–CH_2$ (hydrocarbon group) on the surface of caped CdS. The characteristic peaks due to $–CH_2$ was found to be absent in free CdS. The caped CdS showed a intense peak at 638 cm^{-1} correspond to the stretching vibration of surface stabilized CdS. A large absorption peak corresponding to 3445 cm^{-1} and 1650 cm^{-1} is arising due to the –OH group shows the stretching and bending vibration of the absorbed water on the surface of the CdS while Caped CdS showed characteristic absorption towards lower frequency (3350 $cm^{—1}$). These data indicates the strengthen of band due to C and S of C–S bond on capped surface bonded to S and Cd of CdS after capping. Thus, capping agent confirms the presence of quantum confinement effect in CdS particle.

Figure 5.6b showed SEM micrograph for uncapped CdS and Capped CdS particle. SEM micrograph of uncapped (Free) CdS particle showed aggregation of the particles. However, MPA capped image demonstrate the formation of considerable spherical-shaped nanoparticles with high degree of monodispersion having small size irregularities. The average roughness (12 nm) was detected in AFM image of caped CdS particle. The roughness value lies almost in the range

of size of quantum dots. Thus, capping molecule contributes in the coverage of surface of nanoparticle. The roughness value increases the extent of interfacial contact.

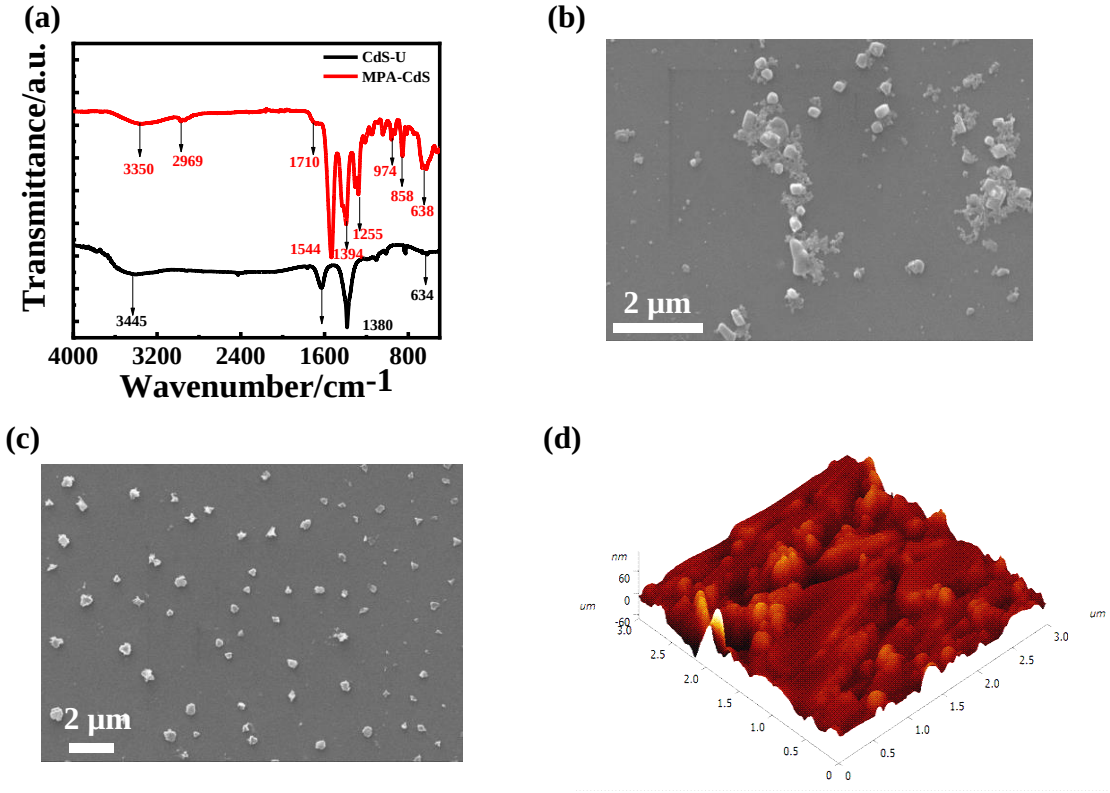

Figure 5.6: (a) Solid state FTIR spectra of free CdS (uncapped) and MPA capped CdS. (b) Fe-SEM image of free CdS (c) Fe-SEM image of MPA capped CdS. (d) AFM image of MPA capped CdS coated on silcon wafer

Figure 5.7a shows the UV-visible absorption spectra of free CdS particle and MPA caped CdS particle. The sharp peak at the wavelength of 268 nm confirms the presence of MPA on CdS particle. The characteristic absorption peak was observed absent in the spectra of free CdS. MPA capped CdS showed blue shifted absorption band (385 nm) confirming the direct consequence of quantum confinement in CdS nanoparticles. Free CdS shows absorption band at 506 nm. Thus, blue shifted absorption features confirming the formation of nanoparticle. The direct bandgap of synthesized CdS NPs was found using the relation, which gives a direct

relationship between optical bandgap (Eg) and wavelength (λ) (i.e., Eg = 1240/λ), where λ is the absorption edge of the material. A plot of $(\alpha hv)^2$ versus (hv) has been used for the determination of the optical energy transition. The optical bandgaps of the CdS nanoparticles prepared with 0.0.65 M MPA concentrations were found to be 2.71eV. The calculated bandgap values were large compared to that of free CdS (Eg = 2.40 eV). The large band gap is direct evidence of size quantization effect

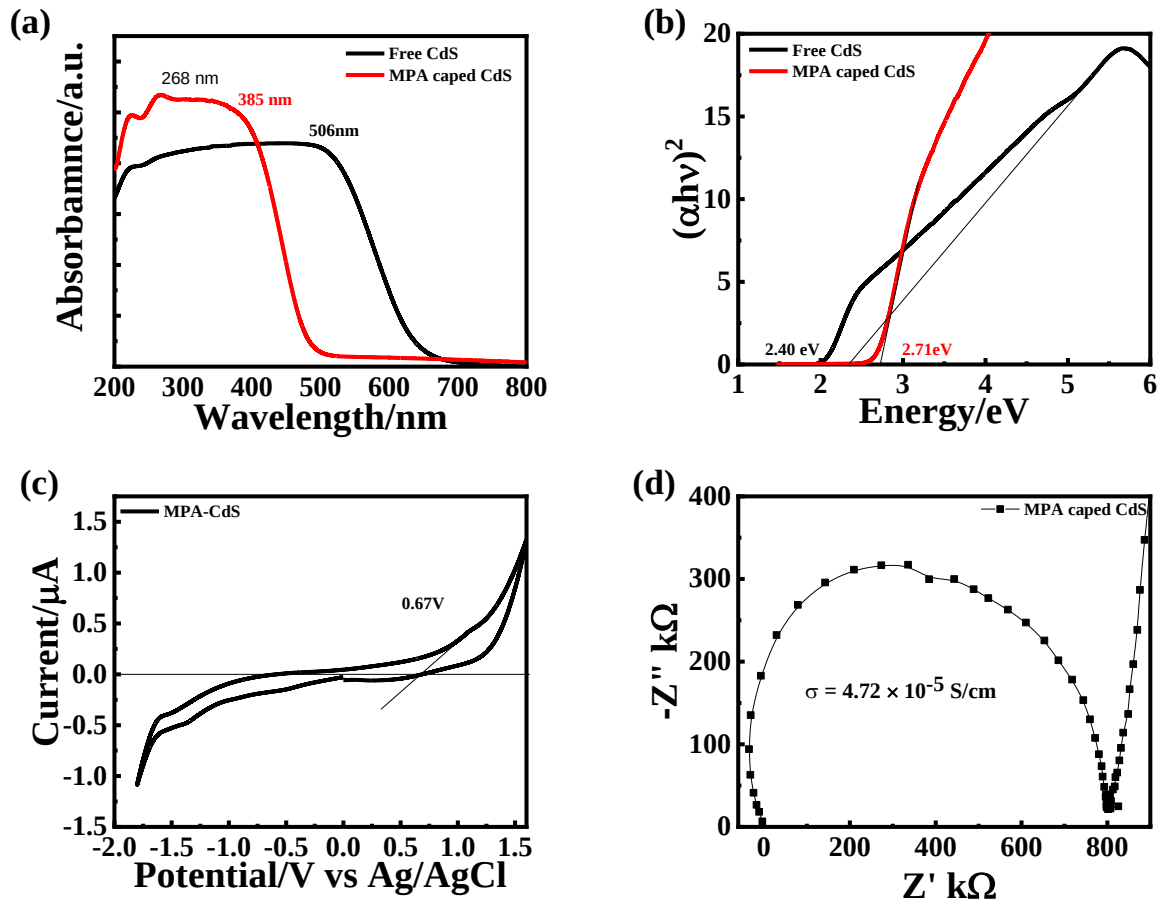

Figure 5.7: (a) Solid state UV-visible absorption spectra of of free CdS and MPA capped CdS. (b) Tauc's plot for determination of band gap through absorption edge transition. (c) dispersed phase cyclic voltammetry (CV) of MPA capped CdS. (d) EIS plot for estimation of electrical conductivity of MPA capped CdS.

Figure 5.7c shows electrochemical characteristic curve of MPA caped CdS particle in dispersed phase. Solution phase cyclic voltammetry was used to characterize redox properties of capped CdS nanoparticles at room temperature. The onset value of oxidation peak was found to occur at 0.67V and onset reduction was at -0.72V. These values are consistent due to relative shifting of VB and CB edges in the nanoparticle due to size quantization effect. Thus, capped CdS particle is electrochemically active.

Figure 5.7d shows the EIS measurements of MPA capped CdS particle in dispersed phase. The charge transfer properties of MPA caped CdS particle can be detected by EIS plot. The appearance of semi-circle indicates the presence of surface conductivity [193]. The electrical conductivity was estimated as 4.72×10^{-5} S/cm due to presence of interfacial layer resistance. Thus, MPA capped CdS particle shows sufficient electrocatalytic activity.

5.4. Interfacial energy levels, band structure and electron injection phenomenon

The energy levels diagram have been shown in **Figure 5.8a, b**. In practice, the photo-generated electrons in FTO substrates can easily recombine with the PUI-electrolyte active group result in the back-transport reaction. The loss of charge recombination can be prevented through optimizing energy levels at the interfacial contacts. Pristine FTO has work function of 4.4 eV. A thin layer of RGO (E_{LUMO} = -2.79eV, E_{HOMO} = - 4.46eV) has been coated on conducting surface of FTO to modify the work function and electron injection density.

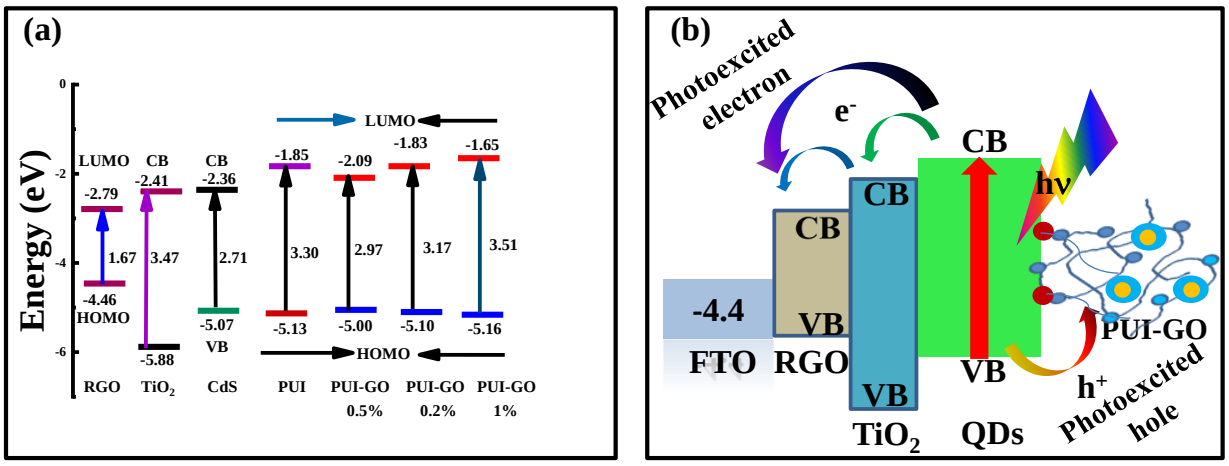

Figure 5.8. (a) Energy levels of constituents materials including polyelectrolyte for assembly of QDSS cells. (b) The possible photoanode electrolyte interface showing increased density of photoexcited electron in FTO for efficient conversion.

Photovoltaic conversion efficiency is due to fast injection of photoexcited electron and photo electrochemical reaction on the surface of redox active pendant anion. Reduced graphene oxide coated electrode (FTO-RGO) may improve the number density of photoexcited electrons in CB and subsequent external circuit for efficient conversion. This is probably attributed to increased electrical conductivity of photoanode. The synergistic interaction of FTO, RGO, TiO_2 and CdS QDs facilitates interfacial transport and prevent direct contact of FTO and electrolyte leading to enhancement of photocurrent-conversion efficiency. The energy level of QDs (VB =-5.07eV) was optimized just below the level of 0.5% GO implanted PUI-GO (E_{HOMO} = -5.00eV) polyelectrolyte. The energy levels are suitable to transfer the hole towards polyelectrolyte. Higher lying LUMO (-2.09 eV) level effectively block the photogenerated electron from QDs to electrolyte active polyurethane ionomer. The high density of hole leads to the oxidation of redox active group because photoanode/electrolyte interface facilitates strong built in potential (internal electric field). Implanted GO can form interconnected channels for conducting reflux electrons (the electrons from external circuit to counter electrode) from Pt counter electrode to the

oxidized conducting gel polyelectrolyte via expanding catalytic area to maintain the reversibility of electrolyte structure and function. Moreover, larger difference between QDs (VB) and Polyelectrolyte (HOMO) may cause depression in hole recovery. The basic nature of the large amount of oxygenic groups in PUI-GO which can anchor on the TiO_2 electrode and result in a variation of the surface potential and hence intensification of photogenerated electron in external circuit.

5.4.1. QDSSCs fabrication and interfacial gel polyelectrolyte activity

Quantum dot sensitized solar cells have been developed via layer (thin film) technology through the combination of photoanode, gel polyelectrolyte and counter electrode. The fabricated FTO/TiO_2/MPA-CdS and FTO-RGO/TiO_2/MPA-CdS work as photoanode which are prone to absorb light. Gel polyelectrolytes (PUI and PUI-GO) were assembled between photoanode and counter electrode (FTO-Pt) to test the solar characteristic curve and performance.

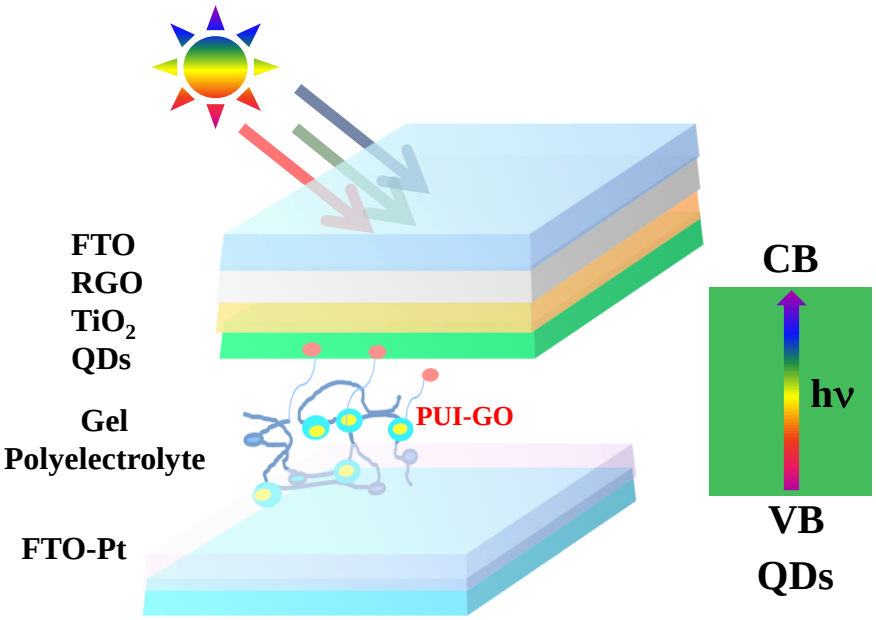

Scheme 5.3: Fabrication of thin film quantum dots sensitized solar cell via insertion of gel polyelectrolyte (PUI-GO) between photoanode and counter electrode

5.5. Photovoltaic performance of QDSSCs using PUI and PUI-GO gel electrolytes

Solar characteristic conversion efficiency was assessed through illumination of photoanode and its synergistic activity with gel polyelectrolytes. **Fig. 5.9a, b** shows the J-V characteristics and power vs voltage plots of QDSSCs with gel polyelectrolytes having different amounts of GO tagged in polyurethane ionomer. RGO coated FTO has ability to fasten the injected electrons from CB of TiO_2 to transport quickly to FTO without back electron transfer.

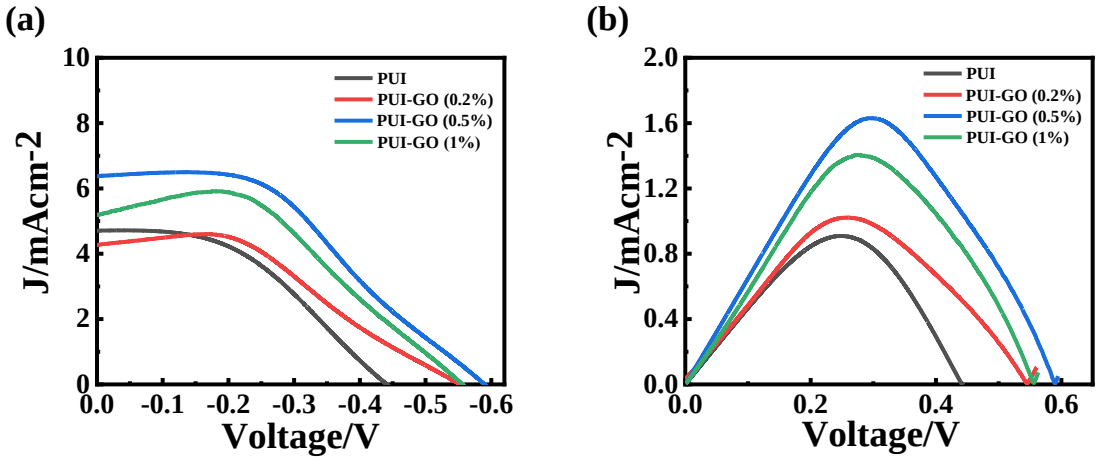

Figure 5.9: (a) J-V solar characteristic measurements of QDSS cells using gel polyelectrolytes with various composition of graphene oxide under the illumination of 100 mW/cm^2 intensity of white neutral LED light. (b) Power vs. Voltage plot to calculate photovoltaic conversion efficiency

Gel Polyelectrolyte	J_{SC} (mA/cm^2)	V_{OC}(V)	FF	P_{max} (mW/cm^2)	η(%)
PUI	4.74	0.442	0.43	0.90	0.90
PUI - GO (0.2%)	4.27	0.549	0.44	1.02	1.02
PUI - GO (0.5%)	6.44	0.594	0.43	1.63	1.63
PUI - GO (1.0%)	5.17	0.560	0.48	1.40	1.40

Table 5.2. Photovoltaic parameters for the measured QDSS cells using gel polyelectrolytes with different composition.

Quantum dots adsorbed photoanode (sintered at 150°C), gel polyelectrolyte and Pt counter electrode (FTO-Pt) were assembled properly for J-V characteristic measurement under solar irradiation having intensity 100 mW/cm^2. Photovoltaic parameters and its value have been enlisted in **Table 5.2**. The photovoltaic cell FTO-RGO/TiO_2/MPA-CdS/PUI/FTO-Pt was

characterized and Photocurrent density (J_{SC} = 4.74 mA/cm^2) and open circuit potential (V_{OC} = 0.442V) were recorded with reasonable conversion efficiency (0.90%). However, GO incorporated polyurethane ionomer gel electrolyte showed elevation in photovoltaic parameters (J_{SC} = 4.27, V_{OC} = 0.549V) and energy conversion efficiency 1.02% which was observed slightly higher than the efficiency 0.90% for pristine PUI activated QDSS cell. Similarly, the power conversion efficiency for the solar cell with conducting gel polyelectrolyte has also been enhanced from 1.02% to 1.63% by utilizing PUI-GO (0.5%) gel polyelectrolyte. The enhancement in efficiency is attributed to the elevation in charge transfer ability and catalytic activity, which can be confirmed by the EIS spectra and tafel plot. The QDSS cell showed enhanced V_{OC} (0.594V) through superior activity of gel polyelectrolyte. The increase in Voc value can be ascribed to the strong coordination ability of carboxylate groups of PUI-GO to metal ions on the surfaces of both TiO_2 and QDs. As a result, the PUI-GO gel, providing a protective layer over the photoanode surface by the steric hindrance effect, can suppress the unfavorable charge recombination process between photoanode and electrolyte [79]. The optimum level of GO facilitates proper orientation to the electrolyte structure which is mainly due to presence of multiple oxygenic center. These oxygenic functional group (electron rich repulsive center) can interact with photoanode and thus hinder the unwanted backward reaction [194]. The high V_{OC} (0.594V) corresponds to PUI-GO (0.5%) showed better electrocatalytic activity as compared to pristine PUI (V_{OC} = 0.442V). The high photocurrent density is due to synergistic extraction of photoexcited electron via RGO and TiO_2 in the device. In other hand, 1w% GO implanted polyurethane ionomer gel showed depression in conversion efficiency (1.40%) of QDSS cell. The reduced efficiency is attributed to slower electrocatalytic activity on the surface of redox active pendant anion. Higher content may aggregate the redox responsive

components leading to depletion of photovoltaic parameter [195]. The chemisorbed dense GO layer will block the electrolyte active sites which probably retard the electrochemical phenomenon and enhance the chance of photoexcited –electrolyte recombination. In addition, excessive GO may weaken the hydrophilicity of polyurethane ionomer resulting in decreased photovoltaic performances in QDSS cell. The photovoltaic open circuit potential was lowered down causing degradation in the characteristic performance of the device. Surface functionality works as conducting interfacial layer. The saturation current densities slightly deviated from steady state and thus, hamper the performance of QDSS cell. Thus, an impressive efficiency of 1.63% was recorded for 0.5% GO implanted PUI. The optimized PUI-GO showed efficient electrolyte activity because of shallow HOMO energy levels and charge transfer characteristics (**Figure 5.8a**). High conversion efficiency is attributed to synergistic catalytic effect in ionomeric segments on the surface of GO and polyurethane chain. Above this amount, it can be demonstrated that high level GO may cause screening and sheath which further degraded the photo electrochemical activity of gel polyelectrolyte.

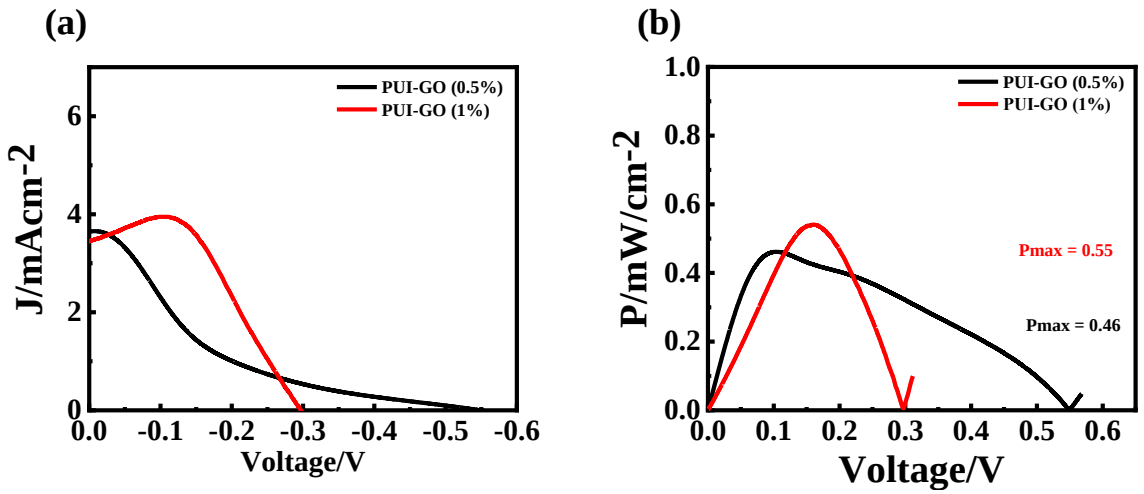

Figure 5.10 (a) Photovoltaic characteristic curves of designed QDSSCs with TiO_2/MPA-CdS/SGO/Gel polyelectrolyte/Pt-FTO configuration (b) Power vs. voltage plot for calculation of conversion efficiency.

On other hand, pristine FTO-TiO_2/MPA-CdS/Gel polyelectrolyte/Pt-FTO and FTO-TiO_2/MPA-CdS/SGO/Gel polyelectrolyte/Pt-FTO configured devices showed poor photovoltaic performance (**Figure 5.10a**). The kind of shrinkage or aggregation might further lower the photocurrent density. The energy conversion efficiency is lowered down confirming slower electrolyte activity (**Figure 5.10b)**. The driving force for charge recombination at the TiO_2/electrolyte interface will become higher with more positive E_{redox} of the electrolyte, and correspondingly leading to faster charge recombination, thus decreasing the photocurrent and photovoltage. The high content of GO more stabilizes the HOMO level (deep energy level) and does not percolate hole mediation efficiently and hence increases the chance of backward charge recombination on polyelectrolyte structure. Thus, high content GO does not suits to polyurethane ionomer and attributed to high energy barrier which further impedes the reversible function of electrolyte between photoanode and photocathode [80]. The tagged carboxylate anion layer could serve as an energetic barrier layer to separate the photogenerated electrons from electrolyte responsive group in the electrolyte and therefore inhibit the charge recombination process in which the photogenerated electrons were captured by the oxidized redox sites in the gel polyelectrolyte [196]. In practice, high GO content probably blocks electroactive sites available on polyurethane chain causing degradation in saturation current density. FTO-RGO/TiO_2/MPA-CdS showed better photocatalytic activity than the pristine FTO-TiO_2/MPA-CdS is because of interfacial Ti-O-C bond formation (TiO_2 have good attraction with epoxy and carboxylate group). This bond formation can increase the interaction area and adsorption of QDs.. The intensive π - stacking repulsion offers suitability to PUI-GO for enhancing energy conversion efficiency.

5.6. Conclusions

In summary, GO has been incorporated to functionalize hard segment content of polyurethane chain. The hydrophilic groups confer stable dispersibility in aqueous or organic solutions by electrostatic repulsions of pendant anions. Optimization of GO content favours the incorporation of pendant anion (electrolyte active group) in polyurethane chain. Hydrophilic pendant group showed complete imbibition in GO implanted polyurethane surface. The tagged GO pendant anion (carboxylate ion) improved charge transport properties via interfacial passivation effect. Composite polyurethane ionomer offered better electrical conductivity as compared to pristine polyurethane ionomer. Photovoltaic effect was realized through synergistic influence of both pendant anions (Carboxylate and sulfonate). Intrinsic polyurethane ionomer (PUI) showed lower photovoltaic activity as compared to composite polyurethane ionomer.. The pendant imbibition intensifies the uniform charge transport. The high energy conversion value is achieved as a result of sufficient conductivity and presence of good contact with the photo-electrode. The short chain organic ligand mercaptopropionic acid (MPA) was found to be an efficient linker on photoanode which accelerates charge transfer process. The increased content of electrolyte active group per unit composite ionomer gel offered elevation in photovoltaic effect. The gel polyelectrolyte activity was found to be suitable at 0.5% of GO content which improves redox activity in polyurethane ionomer. MPA capped CdS Quantum dot sensitized solar cell was successfully developed using PUI-GO (0.5%) with improved photo conversion efficiency of 1.63%. The improved efficiency can be correlated with synergistic activity of GO and polymeric component in polyurethane ionomer. Thus, photovoltaic energy conversion efficiency can be tuned by using appropriate redox active hard segments and chemical composition of polyurethane ionomer. The efficiency enhancement is related to electrolyte structure having expanded electrocatalytic and redox activity.